nanomaterials

Supplementary Materials

Hot Electrons, Hot Holes, or Both? Tandem Synthesis of Imines Driven by the Plasmonic Excitation in Au/CeO_2 Nanorods

Ivo F. Teixeira [1,*], Mauricio S. Homsi [2], Rafael S. Geonmonond [2], Guilherme F. S. R. Rocha [2], Yung-Kang Peng [3], Ingrid F. Silva [4], Jhon Quiroz [5] and Pedro H. C. Camargo [2,5,*]

1 Department of Chemistry, Federal University of São Carlos, São Carlos 13565-905, Brazil
2 Department of Fundamental Chemistry, Institute of Chemistry, University of São Paulo, São Paulo 05508-000, Brazil; mauriciosamuel.homsi@usp.br (M.S.H.); rafaelsg31@gmail.com (R.S.G.); guilhermefrrocha@gmail.com (G.F.S.R.R.)
3 Department of Chemistry, City University of Hong Kong, Yeung Kin Man Academic Building, Hong Kong, China; ykpeng@cityu.edu.hk
4 Department of Chemistry, ICEx, Universidade Federal de Minas Gerais, Belo Horizonte 31270-901, Brazil; ingridfs@ufmg.br
5 Department of Chemistry, University of Helsinki, A.I. Virtasen aukio 1, 00100 Helsinki, Finland; jhon.quiroz@helsinki.fi
* Correspondence: ivo@ufscar.br (I.F.T.); pedro.camargo@helsinki.fi (P.H.C.C.)

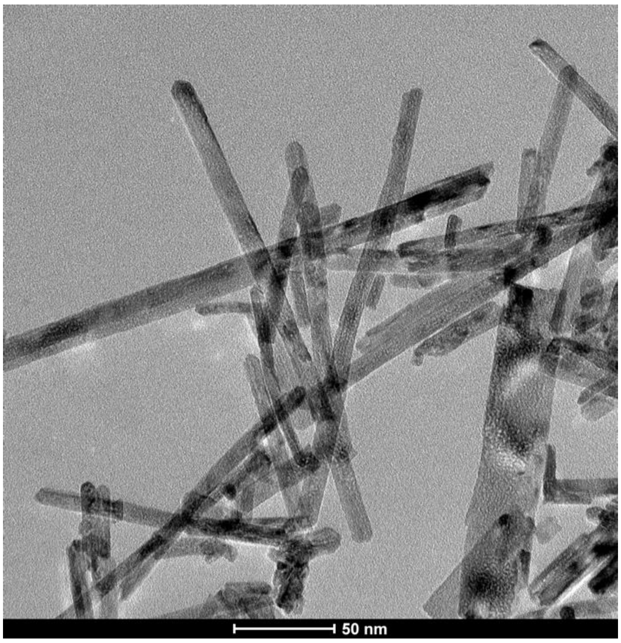

Figure S1. TEM images for the CeO_2 nanorods employed as starting materials for the synthesis of Au/CeO_2 nanorods.

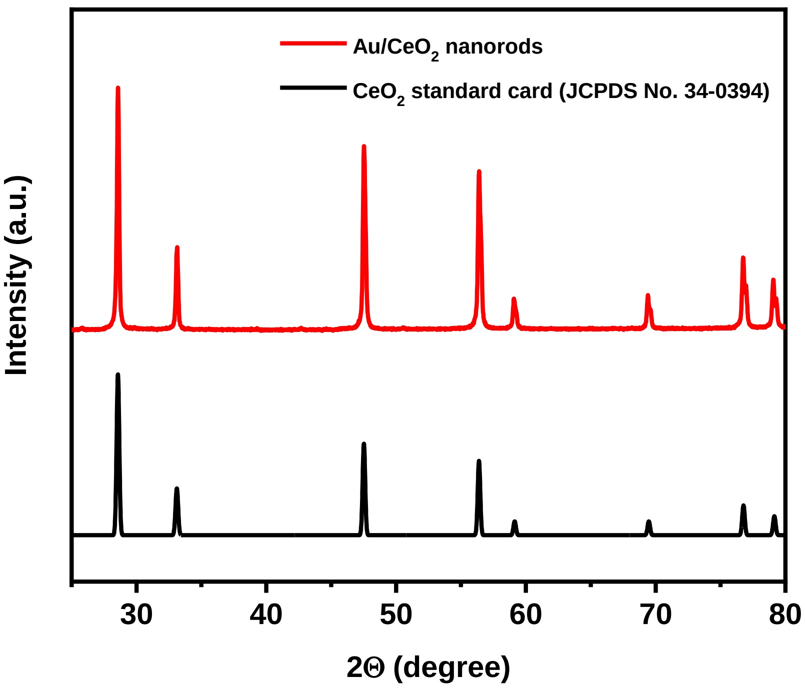

Figure S2. XRD pattern for Au/CeO_2 nanorods. The X-ray diffractometry evidenced the good crystallinity of the sample with peaks assigned to CeO_2 phase.

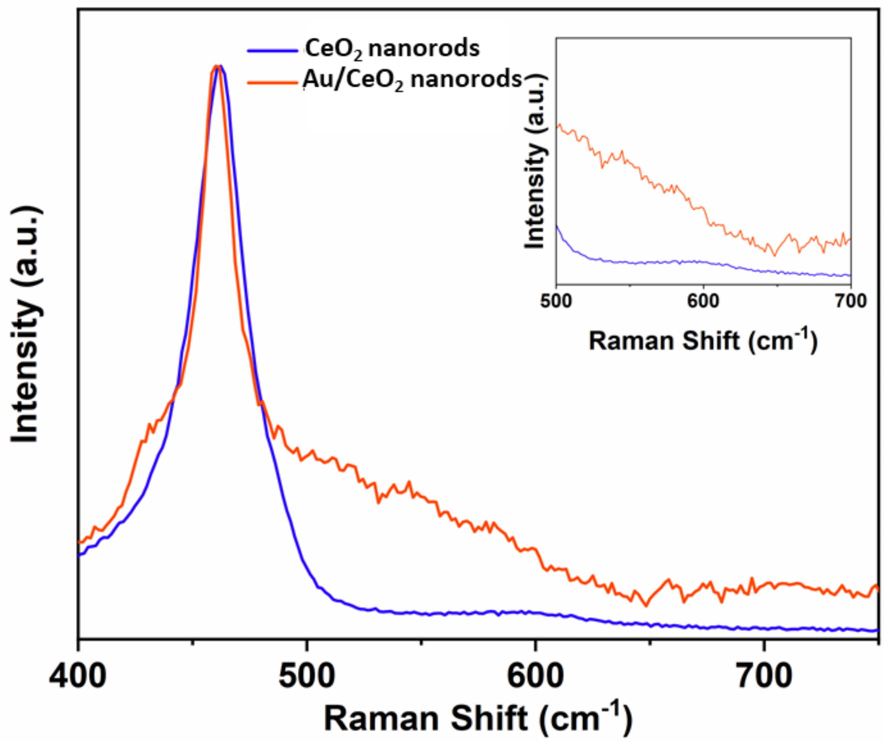

Figure S3. Raman spectra for CeO_2 (blue trace) and Au/CeO_2 (red trace) nanorods. The Raman spectrum of Au/CeO_2 displays a shoulder at 550–600 cm^{-1} assigned to the presence of oxygen vacancies, which is more intense for the Au/CeO_2 nanomaterials relative to the CeO_2 nanorods.

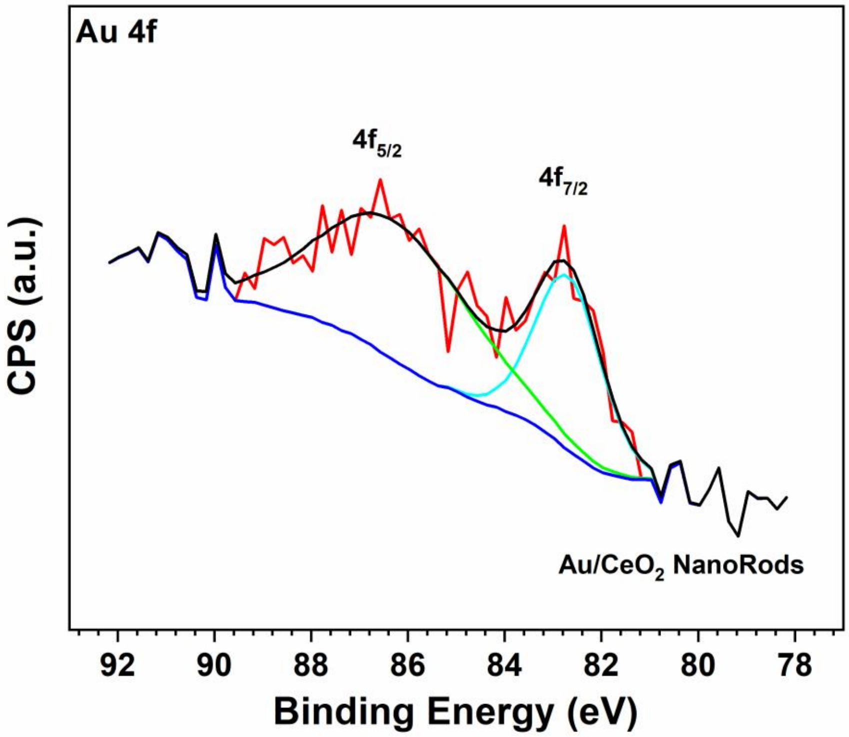

Figure S4. XPS spectra of the Au 4f core-levels for Au/CeO_2 Au/CeO_2 nanorods. It can be observed that for the nanorods, the Au signal is shifted to higher binding energies as a result of stronger metal-support interaction.

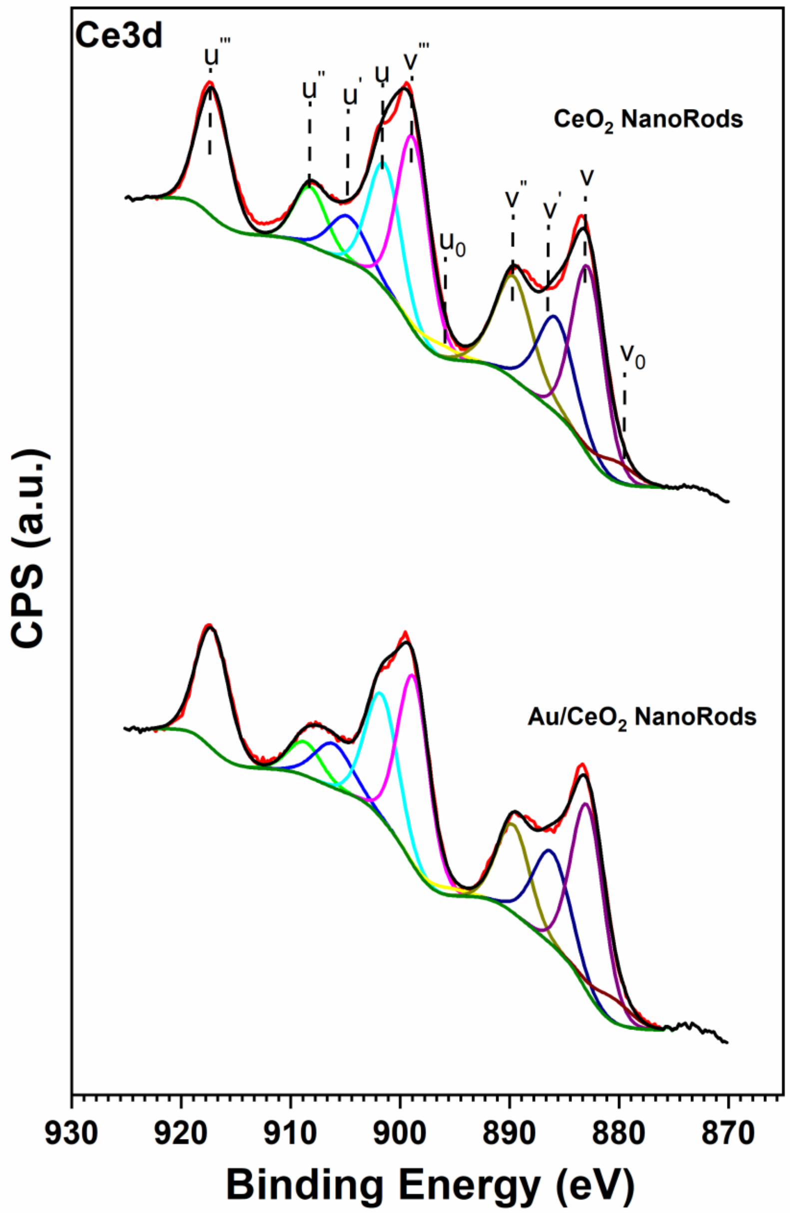

Figure S5. XPS spectra of the Ce 3d core levels for CeO_2 nanorods and Au/CeO_2 nanorods (top to bottom, respectively). No significant differences in the signals for Ce^{3+} and Ce^{4+} species were detected in the samples. They can be associated with different profiles: Ce^{3+} (v_0, v′, u_0 and u′) and Ce^{4+} (v, v″, v‴, u, u″, and u‴). The estimated percentages of Ce^{3+} and Ce^{4+} ions reveal a minimal variance among the samples, suggesting that the addition of low quantities of gold is not promoting the presence of Ce^{3+} and consequently the creation of oxygen vacancies on the cerium oxide as a result of the metal-support interaction [7].

Table S1. Binding energies (eV) of peak positions from Au 4f region and the atomic ratio of Au/Ce for the Au/CeO_2 nanorods.

Sample	$4f_{7/2}$	$4f_{5/2}$	Au/Ce	%at Ce	%at Au
Au/CeO_2 nanorods	82.7	86.3	0.009	99.1	0.9

Table S2. Binding Energy (eV) of O 1s components of samples and relative atomic ratio among species (at. %). Table S2 depicts the BE values obtained from the XPS spectra for the O 1s region for pure CeO_2 and Au/CeO_2 samples, respectively. The signal was deconvoluted into three components located at around 529, 531 and 533 eV (Table S2). These are assigned to lattice oxygen (O_L), oxygen vacancies or surface oxygen ions (O_S), and adsorbed water (O_W), respectively [8]. For all samples, the signal from O_S had the highest contribution with 58% for individual CeO_2 nanorods. After the addition of Au, a slight decrease of the O_S contribution was registered. These results indicate that the enrichment of oxygen vacancies or oxygen ions on the surface of CeO_2 is strongly associated with the shape of the oxide rather than by the addition of Au. It is noteworthy that the Au loading in these samples is very low.

Sample	**O 1s B.E. (at. %)**		
	O_L	**O_S**	**O_W**
Au/CeO_2 nanorods	529.1 (28)	530.8 (45)	533.2 (27)
CeO_2 Nanorods	528.5 (23)	530.4 (58)	532.7 (19)

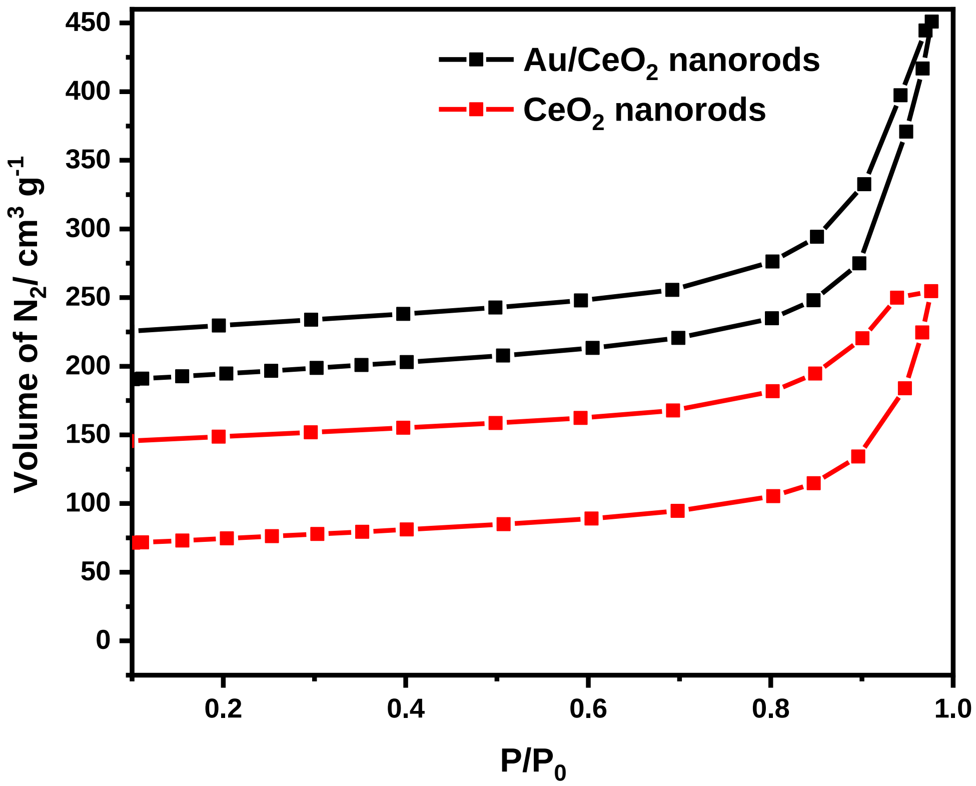

Figure S6. Isotherms BET for CeO_2 nanorods (red trace) and Au/CeO_2 nanorods (black trace). The CeO_2 nanorods samples display a similar porosity and surface area when compared with the Au/CeO_2 nanorods.

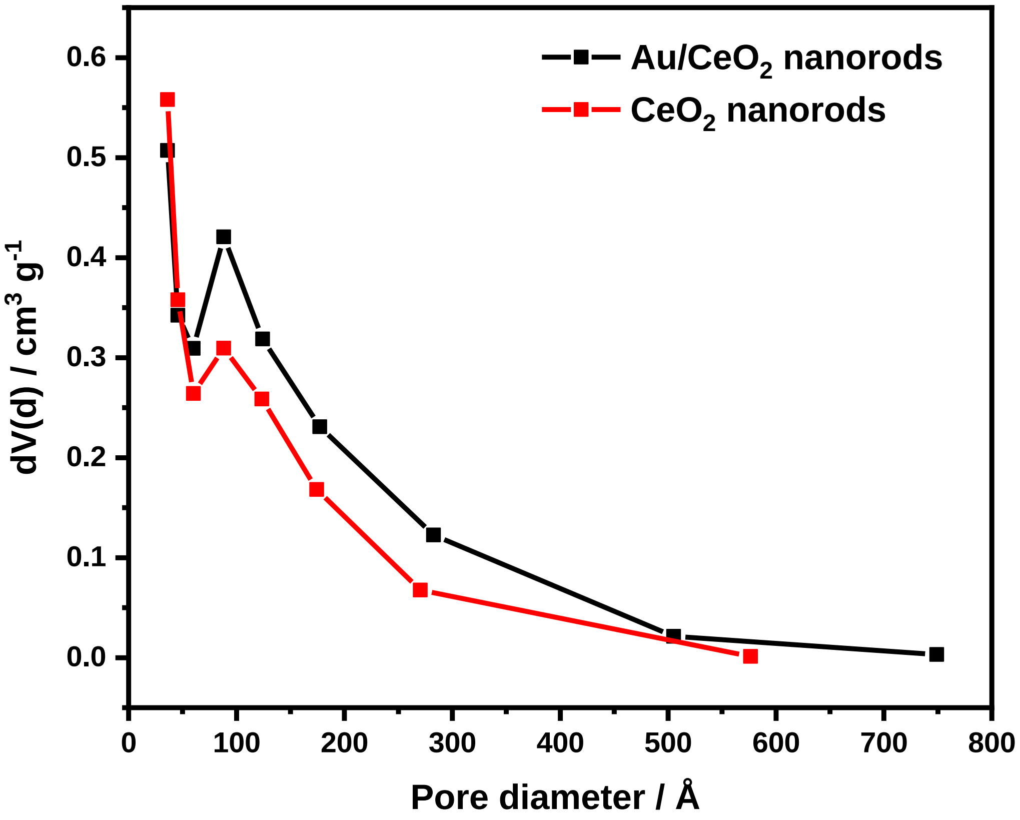

Figure S7. BJH pore diameter distribution for the for CeO_2 nanorods (red trace) and Au/CeO_2 nanorods (black trace). The CeO_2 nanorods samples present mainly mesoporous with larger pores diameters.

Table S3. BET surface area and average pore diameter from Figures S6 and S7.

Sample	Area BET ($m^2 \cdot g^{-1}$)	Pore Diameter (Å)
Au/CeO_2 Nanorods	86.3	177.2
CeO_2 Nanorods	70.6	123.7

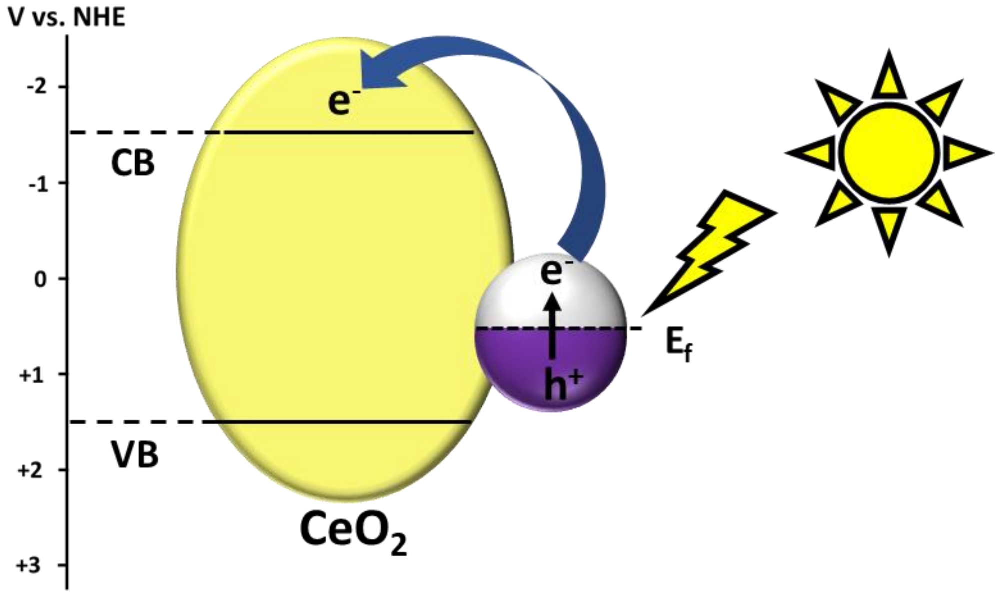

Figure S8. Energy level diagram for the Au/CeO_2 nanorod photocatalyst, illustrating the injection of hot electrons on the conduction band of the CeO_2 and the generation of hot roles in the Au NPs.